

Origin of Chaotic Relaxation Oscillations in an Optically Pumped Molecular Laser

J. V. Moloney, J. S. Uppal,^(a) and R. G. Harrison

Physics Department, Heriot-Watt University, Riccarton EH14 4AS, United Kingdom

(Received 5 March 1987)

We show that pump-induced modifications to the gain and dispersion profiles can induce a weak sideband modulation which acts as a driving term to sustain chaotic relaxation oscillations in a single-mode, resonant, optically pumped molecular laser. Our study suggests that a careful two- or more-parameter unfolding of higher-codimension bifurcations should lead to a wealth of nonlinear dynamical behavior within easy access of current experiments.

PACS numbers: 42.50.Tj, 42.55.Em

Random spiking or sustained relaxation oscillations have been observed in a wide class of lasers from their very inception. However, a clear physical or mathematical explanation of these effects has, with the exception of two cases,^{1,2} remained elusive despite substantial theoretical literature on the topic and recent interest in potentially chaotic laser systems.³ In this Letter we provide a clear physical and mathematical mechanism for sustained chaotic relaxation oscillations in a single-mode, homogeneously broadened laser. Moreover, for our system, an optically pumped molecular laser, we show with a parallel bifurcation analysis that the chaotic motion is associated with a random motion on an attracting set associated with a homoclinic orbit in phase space (double saddle connection). This latter analysis allows us to establish unambiguously (i) a preturbulent regime with eventual collapse onto a stable periodic orbit or cw lasing state, (ii) a chaotic window truncated by the onset of a *pump-induced* stable Rabi sideband oscillation, and (iii) regimes of spontaneous pulsations from both a lasing and nonlasing state.

Optically pumped molecular lasers comprise three levels with the pump and laser transitions sharing a common level, as shown in the inset in Fig. 1(a). Attempts to truncate the equations describing their dynamics to effective two-level systems of the Haken-Lorenz type⁴ involves among others the assumption of a polarization decay rate for the pump transition which is considerably greater than that for the lasing transition,⁵ an unrealistic condition for real molecular systems. Such unphysical truncations are reminiscent of the situation encountered in fluids where the Lorenz equations represent a severe truncation of the original Navier-Stokes equations. In the present laser context the coherent interaction between the pump and lasing emission is suppressed, eliminating the important physics associated with pump-induced Rabi sideband oscillations. In this Letter we emphasize the unique role of the pump laser as a control parameter which, through such coherent interactions, allows one to tailor the gain profile seen by the lasing emission. This unique feature of optically pumped molecular lasers enables us to separate the dynamical features asso-

ciated with the laser emission field from those of the pump field over physical parameter ranges which are well within reach of current experiments.⁶ The present study suggests that much of the rich dynamical behavior of this system remains to be discovered within a careful two- or more-parameter unfolding of higher-codimension

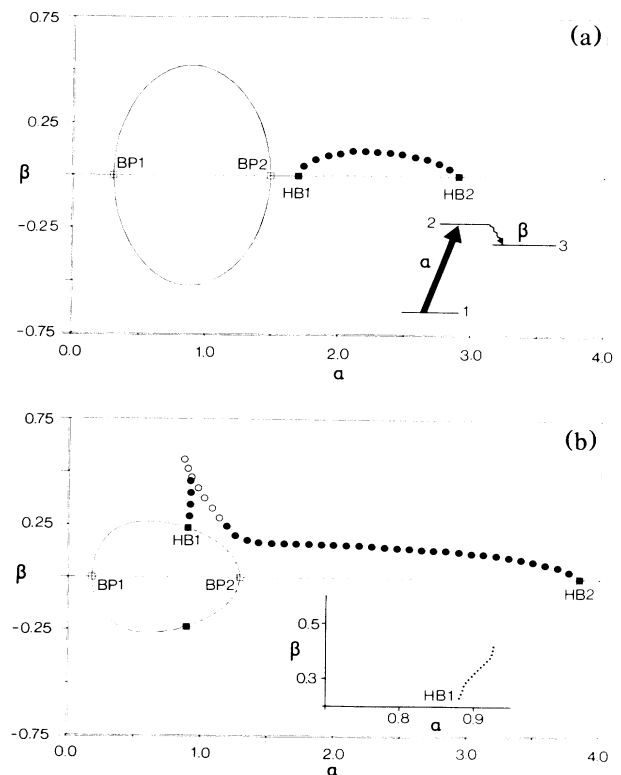


FIG. 1. Bifurcation diagrams for (a) $b=0.8$ and (b) $b=0.2$. Plots show laser-emission amplitude β at line center vs pump amplitude α . The solid lines denote stable cw operation and the dashed lines unstable cw operation; the filled circles are branches of stable periodic solutions and the open circles branches of unstable periodic solutions. Inset in (a): A schematic of the three-level system under study. Inset in (b): A blowup of the region near HB1.

bifurcations.

Our physical model of the optically pumped molecular laser is depicted in the inset in Fig. 1(a). An external-cw-pump laser selectively populates the upper lasing level 2 which can then undergo lasing action to the lower lasing level 3. The equations describing laser action are a simple generalization of the semiclassical equations of Sargent, Scully, and Lamb⁷ to a three-level system. They are derived by coupling of the classical Maxwell electromagnetic field equations to the three-level density-matrix equations and imposition of a self-consistency requirement. The result for the general detuned case is the following set of coupled ordinary differential equations:

$$\begin{aligned}\dot{\beta} &= -(\sigma\beta + ig\rho_{23}), \\ \dot{\rho}_{21} &= -(1 - i\delta_p)\rho_{21} + iaD_{21} - i\beta\rho_{31}, \\ \dot{\rho}_{23} &= -(1 - i\delta_s)\rho_{23} + i\beta D_{23} - ia\rho_{31}^*, \\ \dot{\rho}_{31} &= -[1 + i(\delta_p + \delta_s)]\rho_{31} - i\beta^*\rho_{21} + ia\rho_{23}^*, \\ \dot{D}_{21} &= -b(1 + D_{21}) - 4\text{Im}(\alpha^*\rho_{21}) - 2\text{Im}(\beta^*\rho_{23}), \\ \dot{D}_{23} &= -bD_{23} - 2\text{Im}(\alpha^*\rho_{21}) - 4\text{Im}(\beta^*\rho_{23}).\end{aligned}$$

Here β refers to the complex lasing field amplitude, ρ_{ij} are the off-diagonal density-matrix elements representing atomic coherences, and D_{ij} refer to the pump and laser signal population inversions. The pump-laser amplitude α is assumed constant, g the unsaturated gain is dependent upon the lasing-material properties, σ is the cavity damping constant, and $b = \Gamma/\gamma$ measures the ratio of energy to dipole relaxation rates; δ_p and δ_s refer respectively to the detunings of the pump (1-2) and generated laser emission (2-3) from line center [see inset in Fig. 1(a)]. All parameters are normalized to the dipole decay width (γ) and the dimensionless time is in units of this latter parameter. We assume for simplicity that the dipole decay rates for each off-diagonal density-matrix element are equal (γ) and that the energy relaxation rates for each atomic level are also equal (Γ). In the following, we assume that the pump laser is resonant with transition 1-2 and fix the unsaturated gain $g = 50$ and the cavity loss $\sigma = 10$.

Partial results from an extensive bifurcation analysis of the above system of ordinary differential equations are given in Fig. 1 for the simplest case of an on-resonant pump ($\delta_p = 0$) and laser line-center emission ($\delta_s = 0$). The nature of the global dynamics of the equations is a sensitive function of the magnitude of the parameter b . For b close to unity the bifurcation behavior is simple, as shown in Fig. 1(a) for $b = 0.8$. As the external pump amplitude is increased the system undergoes a pitchfork bifurcation from a nonlasing to a cw (steady) lasing state (BP1) at $\alpha = 0.3$. This is simply the first laser threshold. With stronger pumping, the lasing-emission amplitude initially grows and then begins to drop off

rather rapidly and the laser eventually turns off (BP2) at $\alpha = 1.48$. At higher pump amplitude ($\alpha = 1.69$), the laser again turns on via a Hopf bifurcation (HB1) to a stable periodic oscillation [branch in Fig. 1(a) denoted by filled circles] which dies out at larger α ($= 2.9$) (reverse Hopf bifurcation at HB2).

The effect of decreasing the parameter b is shown in Fig. 1(b), where at $b = 0.2$ the left-hand Hopf bifurcation point (HB1) at $\alpha = 0.9$ has migrated to the left and onto the lasing branch. This movement to smaller α is smooth as a function of decreasing b . The Hopf bifurcation point, now on the lasing branch, is commonly referred to as the second lasing threshold. A simple calculation shows that the frequency at this Hopf bifurcation point is nearly coincident with the natural relaxation oscillation frequency ω_{rel} of the laser. The branch of periodic solutions emanating from the Hopf bifurcation point is denoted by filled circles when stable and by open circles when unstable. The periodic branch is now more complicated containing a finite region of pump amplitude α where no stable solutions appear. This narrow window in α ($0.905 < \alpha < 1.145$) corresponds to the chaotic lasing region. A blowup of the periodic branch near the leftmost Hopf bifurcation point is shown as an inset in Fig. 1(b). In contrast to the Lorenz model, the bifurcation here is supercritical with the stable limit cycle losing stability at the limit point (change to open circles) and the resulting period of the unstable limit cycle rapidly increasing with decreasing α . This suggests that a branch of homoclinic bifurcations should exist in a two-parameter unfolding. We have in fact located an unstable periodic orbit of large period (period=2040) which comes very close to the unstable saddle (nonlasing state). Full details of this analysis will be published elsewhere. The limit point at $\alpha = 0.905$ on the branch of periodic solutions in Fig. 1(b) (see inset) marks the onset of chaotic random spikings. The narrow region between HB1 and this limit point is the preturbulent region where initial random spikings are eventually trapped on the stable limit cycle. Below HB1, a preturbulent regime exists where eventual collapse occurs onto the stable lasing state. The point ($\alpha = 1.145$) where the chaotic window ends corresponds to the change from unstable to stable limit-cycle behavior on the periodic branch. This latter branch eventually terminates on the nonlasing branch at $\alpha = 3.84$ (HB2).

The physical picture of the periodic and chaotic motion can be understood from the plots of the laser output amplitude and the corresponding cavity dispersion curves versus normalized detuning, as shown in Fig. 2 for $b = 0.2$. Immediately above threshold at $\alpha = 0.18$, the laser-emission profile is single humped and the corresponding dispersion is characteristically anomalous. The dip in the emission profile and strong modification of dispersion near line center at $\alpha = 0.9$ [HB1 in Fig. 1(b)] result from pump-induced Rabi splitting of states 1 and

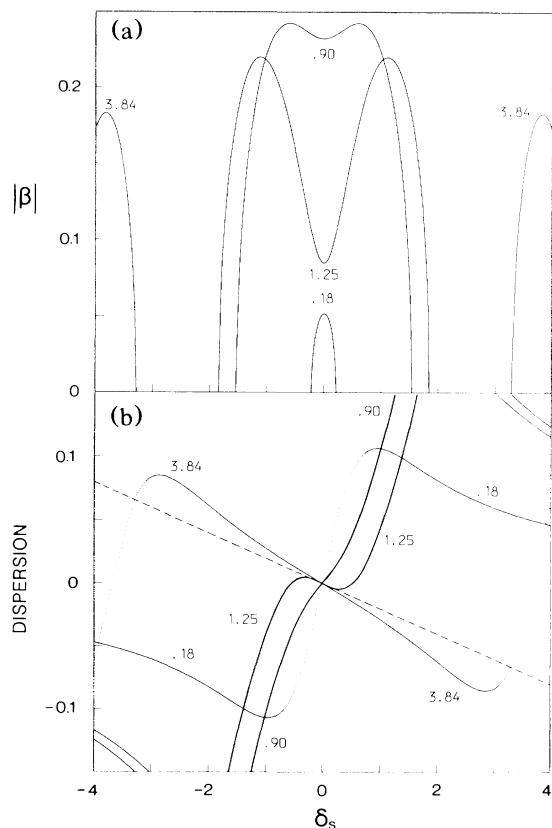


FIG. 2. (a) Modulus of the laser amplitude β and (b) cavity dispersion relation against laser signal detuning δ_s for $b=0.2$. The laser amplitude β at $\delta_s=0$ coincides with the branch of steady-state solutions in Fig. 1(b).

2. At $\alpha=1.25$, two new intersections appear with the straight cavity line suggesting the possibility of sideband oscillation.⁸ The preceding bifurcation analysis, however, shows that stable oscillation occurs just beyond $\alpha=1.145$ terminating the chaotic oscillation. Sideband oscillation frequencies determined from the dispersion analysis agree with the exact predictions of the bifurcation analysis for large α (≥ 2) but deviate for low α ($\sim 15\%$ for $\alpha=1.5$) where the small-signal treatment implicit to the former analysis is approximate.⁹ This accounts for the slight deviation between values of α (1.145 and 1.25) for the transition to sideband oscillation from the two treatments. The line-center laser emission drops below threshold at $\alpha=1.29$, as shown in Fig. 1(b). The transition from low-amplitude oscillation to nonlasing state at $\alpha=3.84$ [HB2 in Fig. 1(b)] is accurately captured in Fig. 2(b) where the double-humped gain region has just shifted outside the cavity dispersion curve intersection line.

The physical picture of the chaotic motion is now clear. The pump laser induces a strong distortion in the gain (inverted dip at line center) and dispersion charac-

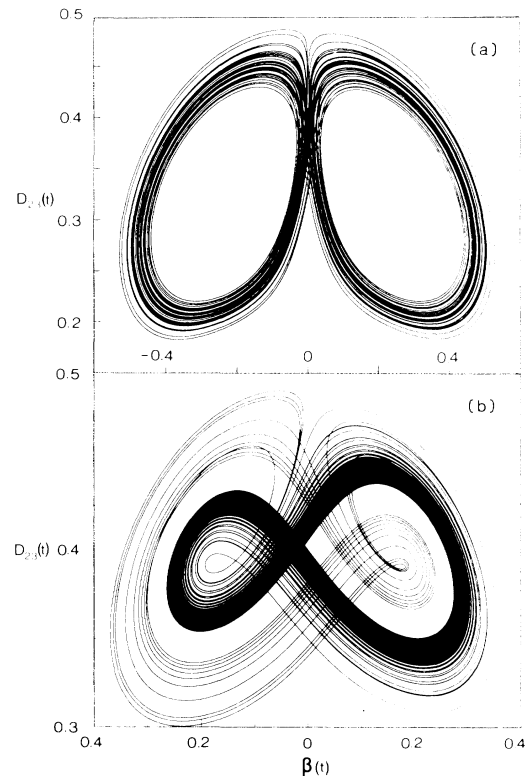


FIG. 3. Trajectories showing graphs of the laser inversion $D_{23}(t)$ vs laser-emission amplitude $\beta(t)$ at (a) $\alpha=0.908$ and (b) $\alpha=1.14$ in the chaotic region of Fig. 1.

teristics of the homogeneously broadened laser line leading to a dynamic modulation which can sustain the laser relaxation oscillation. With further increase in pumping a sharp transition occurs from periodic relaxation oscillations directly to chaotic motion. A sharp return to stable Rabi sideband oscillations occurs at larger pump amplitude as a consequence of the appearance of new side modes resonant with the cavity frequency. The differing chaotic-attractor topologies evident in Fig. 3 reflect the physically distinct processes operative in the laser at different pumping levels. At $\alpha=0.908$ [Fig. 3(a)] the chaotic motion involves unstable outward spiraling mimicking the motion in the neighborhood of the nearby unstable limit cycle. This motion is confined predominantly within the positive and negative amplitude lobes defined by the stable and unstable manifolds of the nonlasing saddle point ($\beta=0$ in Fig. 1) and manifests itself physically in the intensity dynamics as random large-amplitude excursions followed by ringing oscillations. At larger pumping ($\alpha=1.0$) the chaotic motion in Fig. 3(b) occurs about an unstable Rabi sideband limit cycle giving rise to a symmetric (about $\beta=0$) chaotic attractor. Intensity outputs now occur as sequences of pulses with intensities frequently dropping close to zero lasing intensity. Both of these types of dynamical pulsations are

characteristics of a wide variety of unstable laser systems irrespective of the physical mechanism responsible for oscillation.

The ease with which the Hopf bifurcation points HB1 and HB2 can be translated along the branches of steady-state solutions by the variation of either b or the cavity loss indicates that branches of homoclinic orbits can be tracked under two- or more-parameter unfoldings.¹⁰ A wealth of chaotic scenarios associated with homoclinic bifurcations then becomes possible.

The authors thank A. Vass for stimulating discussions. This work has been supported through Science Research Council (GR/D/68627). One of us (J.V.M.) is indebted to E. Doedel for providing the AUTO bifurcation package.

^(a)On leave from the Laser Division, Bhabha Atomic Research Centre, Bombay, India.

¹J. A. Fleck, Jr., and R. D. Kidder, *J. Appl. Phys.* **35**, 2825 (1964).

²L. W. Casperson, *J. Opt. Soc. Am. B* **2**, 62–80 (1985); L. W. Casperson and A. Yariv, *IEEE J. Quantum Electron.* **8**, 69 (1972).

³A recent review of laser instabilities can be found in the special issue on Instabilities in Active Optical Media, *J. Opt. Soc. Am. B* **2** (1985). A detailed analysis of mode splitting in a two-level system is given by S. T. Hendow and M. Sargent, III, *J. Opt. Soc. Am. B* **2**, 84–101 (1985); see also Ref. 2.

⁴H. Haken, *Phys. Lett.* **53A**, 77 (1975).

⁵M. A. Dupertuis, R. R. E. Salomaa, and M. R. Siegrist, *Opt. Commun.* **57**, 40 (1986).

⁶C. O. Weiss and J. Brock, *Phys. Rev. Lett.* **57**, 2804 (1986).

⁷M. Sargent, III, M. O. Scully, and W. E. Lamb, Jr., *Laser Physics* (Addison-Wesley, Reading, MA, 1974).

⁸S. C. Mehendale and R. G. Harrison, *Phys. Rev. A* **34**, 1613 (1986).

⁹J. S. Uppal, R. G. Harrison, and J. V. Moloney, *Opt. Commun.* (to be published).

¹⁰J. Guckenheimer and P. Holmes, in *Nonlinear Oscillations, Dynamical Systems, and Bifurcations of Vector Fields*, Applied Mathematical Sciences, Vol. 42, edited by F. John, L. Sirovich, and J. P. LaSalle (Springer-Verlag, New York, 1983).